Optical study of a doubly negatively charged exciton in a CdTe/ZnTe quantum dot containing a single Mn^{2+} ion

T. Smoleński,[1,*] M. Koperski,[1] M. Goryca,[1] P. Wojnar,[2] P. Kossacki,[1] and T. Kazimierczuk[1]
[1]*Institute of Experimental Physics, Faculty of Physics, University of Warsaw, ul. Pasteura 5, 02-093 Warsaw, Poland*
[2]*Institute of Physics, Polish Academy of Sciences, Al. Lotników 32/64, 02-688 Warsaw, Poland*
(Received 31 May 2015; revised manuscript received 16 July 2015; published 13 August 2015)

We present a magnetospectroscopic study of a doubly negatively charged exciton X^{2-} in a CdTe quantum dot doped with a single Mn^{2+} ion. The X^{2-} emission leading to the singlet final state of an excited electron pair is demonstrated to consist of six distinct lines corresponding to different projections of the Mn^{2+} spin, similarly as for the neutral exciton X. We show that the fine structure of X^{2-} energy levels, as well as the effects of the longitudinal magnetic field, are well reproduced by a simple spin Hamiltonian model featuring both carrier-ion and intershell electron-hole exchange interactions. We also point out two important effects distinguishing the X^{2-} from the X, which result from different symmetries of the electron wave function: the field-induced decrease of the anisotropic part of intershell electron-hole exchange, and the negligible value of the Mn^{2+} exchange integral with the *p*-shell electron.

DOI: 10.1103/PhysRevB.92.085415 PACS number(s): 71.70.Gm, 78.67.Hc, 75.75.−c, 78.55.Et

I. INTRODUCTION

The exchange interaction in semiconductor quantum dots (QDs) is an important factor governing the fine structure of excitonic energy levels, and thus influencing the optical properties of the QDs. The most basic example is the exchange coupling between an electron and a hole forming the neutral exciton (X). Numerous studies of different QD systems [1–4] established a universal description of this exchange interaction, which is defined by two contributions: the isotropic contribution, which is responsible for δ_0 splitting of bright and dark excitonic states, and the anisotropic contribution, which leads to δ_1 splitting of two bright states. The latter part of the electron-hole exchange is known as the main factor hindering the entanglement between the photons emitted during cascaded biexciton recombination [5–7]. Consequently, the control of the magnitude of this interaction attracted a lot of scientific attention, resulting in several successful experimental demonstrations of entanglement between the photons emitted from a single QD [8–10].

A qualitatively different type of the exchange interaction arises in the QDs containing single transition metal ions [11–13]. In this case, both the electron and the hole interact with a localized spin of a magnetic impurity via the *s*, *p*-*d* exchange [14]. One of the consequences of such an interaction is the possibility of optical control of the ion spin state. It was demonstrated in several previous experiments, which uncovered, e.g., that the ion spin can be optically oriented [15–19] and its coherent evolution may be directly probed by means of a time-resolved measurement of absorption of a single dot [20]. All of these studies were focused mainly on the neutral exciton. The exchange interaction between this complex and the ion is governed mostly by the hole-ion interaction, which, given the heavy-hole character of the excitonic ground state, is Ising-like [11]. As a result, the X emission is split into $2S + 1$ lines, each corresponding to a different projection of the ion spin *S* onto the hole anisotropy axis (i.e., the growth axis) [11–13]. In the particular case of a CdTe/ZnTe QD with a single Mn^{2+} ion ($S = 5/2$), the excitonic photoluminescence (PL) spectrum thus exhibits a well-established sixfold splitting [11,21–25]. The PL studies of the other excitonic complexes in magnetic QDs have received much less research attention so far. In particular, they were solely limited to the complexes consisting of carriers occupying only the orbital ground states (i.e., *s* shell). The effects related to the exchange interaction between the ion and carriers in the excited orbital states (e.g., *p* shell) have been studied theoretically [26,27]. In particular, the authors of Ref. [27] found that excitonic complexes containing a large number of electrons ($\geqslant 3$) may be used as a convenient probe of the exchange interaction between the *p*-shell electron and the Mn^{2+} ion.

In this work, we present a detailed magneto-optical study of a doubly negatively charged exciton (X^{2-}) in CdTe/ZnTe QDs containing single Mn^{2+} ions. Such an excitonic complex is one of the simplest, which contains at least one *p*-shell electron in its ground state. Experimentally, we analyze the X^{2-} emission to the final state corresponding to the excited electron pair forming a singlet configuration. Due to the strong exchange interaction between these electrons [28], such emission lines are well-separated from the other lines visible in the PL spectrum of a CdTe QD. Our findings reveal that in contrast to the theoretical predictions from Ref. [27], the fine structure of the X^{2-} emission is governed not only by the carrier-ion exchange, but it is also strongly influenced by the exchange interaction between the *p*-shell electron and the *s*-shell hole. We demonstrate that the properties of the X^{2-} PL spectrum as well as its evolution in a longitudinal magnetic field can be accurately reproduced within a frame of a spin Hamiltonian model. On this basis, we show that the exchange integral between the Mn^{2+} ion and the *p*-shell electron is much smaller compared to the integral for the *s*-shell electron, which is independently determined from the analysis of the neutral exciton PL. Due to the presence of a single ion in the dot, our results also provide insight into the properties of the X^{2-} complex itself. In particular, we demonstrate that the anisotropic part of the exchange interaction between the

*Tomasz.Smolenski@fuw.edu.pl

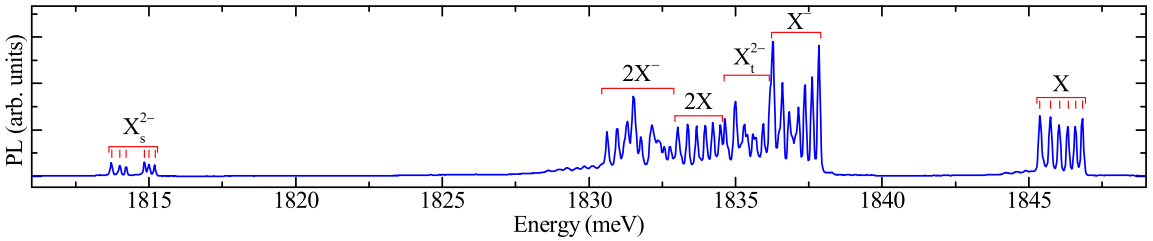

FIG. 1. (Color online) PL spectrum of a CdTe/ZnTe QD (denoted as QD1) containing an individual Mn^{2+} ion. The spectrum was measured without polarization resolution. The sixfold split emission line labeled as X_s^{2-} is related to the recombination of X^{2-} to the singlet configuration of the excited electron pair.

s-shell hole and the *p*-shell electron is significantly decreasing upon application of a magnetic field.

II. SAMPLE AND EXPERIMENTAL SETUP

The sample studied in this work was grown by molecular beam epitaxy. It consists of a single layer of self-assembled CdTe/ZnTe QDs doped with Mn^{2+} ions. The Mn^{2+} concentration was adjusted to assure high formation probability of QDs containing exactly one Mn^{2+} ion. The magneto-optical measurements of individual QDs were carried out in a micro-PL setup on a sample placed inside a helium bath cryostat ($T = 1.8$ K). A reflective-type microscope objective was attached directly to the sample surface to assure high spatial resolution of both PL excitation and detection. The cryostat was equipped with a superconducting magnet producing a magnetic field of up to 10 T. The field was applied in Faraday geometry along the growth axis of the sample. The QDs were excited nonresonantly using either a 405 or a 532 nm continuous-wave diode laser. The PL from the dots was resolved using a 0.5 m monochromator and recorded with a CCD camera.

III. FINE STRUCTURE OF X^{2-} IN Mn-DOPED QD

The experiments revealing the fine structure of X^{2-} in a QD with a single Mn^{2+} ion were performed on a number of Mn-doped dots. The PL spectrum of a representative one (denoted later as QD1) is shown in Fig. 1. As the dominant excitation channel of a nonresonantly pumped CdTe QD corresponds to single carrier trapping [29], we observe emission lines related to the excitonic complexes of different charge states. Each of them exhibits multifold splitting induced by the carrier–ion exchange interaction. The sequence and relative energies of the consecutive groups of exchange-split lines are found to be similar to those previously reported for nonmagnetic CdTe QDs [24,25,28,30]. On this basis, as well as on the basis of exchange-related splitting patterns, the groups of lines were identified as originating from the recombination of a neutral exciton (X), a negatively charged exciton (X^-), a doubly negatively charged exciton (X^{2-}), a neutral biexciton (2X), and a negatively charged biexciton ($2X^-$). As seen in Fig. 1, the X^{2-} PL consists of two distinct sets of lines labeled as X_t^{2-} and X_s^{2-}, which correspond to different spin configurations of the excited electron pair forming the final state of the X^{2-} recombination [28,31–35]. The high-energy set of lines (X_t^{2-}) is related to the recombination to the two-electron triplet states, while the low-energy set (X_s^{2-}) corresponds to the case in which the remaining electrons are in the singlet configuration. The energy distance between these two sets of lines, which is defined by the electron-electron exchange integral $2J_{ee}$, yields about 21 meV for the studied QD. This value is consistent with $2J_{ee}$ of (20.4 ± 1.4) meV determined in Ref. [28] based on systematic studies of nonmagnetic CdTe QDs. Such an agreement additionally confirms the correct identification of both groups of X^{2-} transitions.

The detailed studies of X^{2-} recombination to the triplet final states are hindered, since the corresponding emission energies partially overlap with the energies of 2X and X^- optical transitions. In the following, we will thus focus on a well-separated group of lines related to the X^{2-} emission to the singlet final state. Such a final state is degenerate with respect to the ion spin, since the electrons forming a singlet configuration do not interact with the ion. As a result, the energies of emission lines within the investigated X_s^{2-} group are defined only by the energy spectrum of the X^{2-}. Such a complex consists of a single *s*-shell hole and three electrons. One of them is placed in the *p* shell, while the other two electrons are accommodated in the closed *s* shell and do not interact with the remaining carriers, nor with the magnetic ion. Thus, the X^{2-} fine structure is governed by the exchange interaction between the *s*-shell hole, the *p*-shell electron, and the Mn^{2+} ion. As a consequence, there is a close analogy between the X^{2-} and the neutral exciton, for which the energy spectrum is defined by the same exchange interactions, except that an electron forming the X resides on the *s* shell. Moreover, in both cases the final state of the recombination (two-electron singlet or an empty QD) is degenerate. Altogether, this results in similar emission patterns of X_s^{2-} and X, each consisting of six almost equally intense emission lines (see Fig. 1). Apart from these similarities, there are also substantial differences between the two PL spectra resulting from different symmetries of the electron wave function. In particular, the X_s^{2-} emission lines are not uniformly spaced with a pronounced gap between the two sets of three lines.

To provide a quantitative description of all observed features of the X^{2-} emission, we introduce a simple model of X^{2-} in a Mn-doped QD based on the general spin Hamiltonian

$$H_{X^{2-}} = H_{\text{exch}}^{e\text{-}h} + H_{\text{exch}}^{\text{ion}} + H_{\text{conf}}, \tag{1}$$

where $H_{\text{exch}}^{e\text{-}h}$ describes the exchange interaction between a *p*-shell electron and an *s*-shell hole, $H_{\text{exch}}^{\text{ion}}$ corresponds to the carrier-ion exchange, and H_{conf} accounts for higher-order effects related to the configuration mixing [21,36,37].

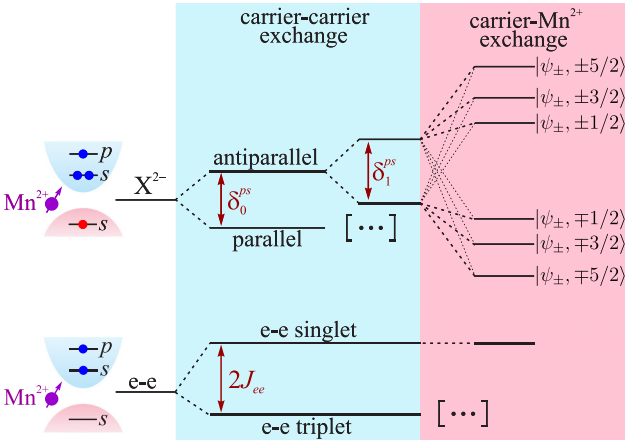

FIG. 2. (Color online) The scheme of energy levels corresponding to initial and final states of the X^{2-} recombination in Mn-doped QD. Note that the level spacing is not in scale.

Following the previous studies of CdTe QDs [28,30], we assume that the degeneracy of two p orbitals is lifted (possibly due to in-plane anisotropy of the QD), and we take into account only the lowest-energy p orbital.

We first analyze the effects of intershell electron-hole exchange leaving out the ion spin degree of freedom. Similarly to the case of the neutral exciton, such an interaction can be described by taking into account both isotropic and anisotropic contributions in the effective Hamiltonian [28,33–35]:

$$H_{\text{exch}}^{e\text{-}h} = -\frac{2}{3}\delta_0^{ps}\sigma_z^p J_z^s + \frac{\delta_1^{ps}}{3}\left(\sigma_x^p J_x^s + \sigma_y^p J_y^s\right), \qquad (2)$$

where $\vec{\sigma}^p$ is the p-shell electron spin operator, while $\vec{J}^s$ is the s-shell hole pseudospin operator represented in the two-dimensional subspace of low-energy heavy-hole states. The latter operator might be expressed using the Pauli matrices $\vec{\tau}$ as $\vec{J}^s = \frac{3}{2}\vec{\tau}$. The isotropic part of the $H_{\text{exch}}^{e\text{-}h}$ splits four spin states of the X^{2-} complex into two subspaces separated by the energy of δ_0^{ps}, as schematically depicted in Fig. 2. The higher-energy subspace consists of two states corresponding to antiparallel spin orientation of the p-shell electron and the s-shell hole, while the lower-energy subspace is composed of the states corresponding to parallel alignment of the spins of both carriers. The anisotropic part of intershell electron-hole exchange lifts the degeneracy between two antiparallel states and splits them by δ_1^{ps} into linear combinations of the form $\frac{1}{\sqrt{2}}(|\begin{smallmatrix}\downarrow\\ \uparrow\downarrow\end{smallmatrix}\Uparrow\rangle \pm |\begin{smallmatrix}\uparrow\\ \uparrow\downarrow\end{smallmatrix}\Downarrow\rangle)$ (see Fig. 2). Here we have adopted the notation from Ref. [28], where $\uparrow$, $\downarrow$ and $\Uparrow$, $\Downarrow$ represent $\pm 1/2$ electron spin and $\pm 3/2$ hole spin, respectively, while $|\begin{smallmatrix}P_e\\ S_e\end{smallmatrix} S_h\rangle$ denotes the state with a P_e electron on the p shell, an S_e electron(s) on the s shell, and an S_h hole on the s shell. According to the optical selection rules, the s-shell hole can only recombine with the s-shell electron provided that both carriers have antiparallel spins. As a result, the recombination of the parallel X^{2-} states ($|\begin{smallmatrix}\uparrow\\ \uparrow\downarrow\end{smallmatrix}\Uparrow\rangle$ and $|\begin{smallmatrix}\downarrow\\ \uparrow\downarrow\end{smallmatrix}\Downarrow\rangle$) leads to the triplet states of the excited electron pair ($|\begin{smallmatrix}\uparrow\\ \uparrow\end{smallmatrix}\rangle$ and $|\begin{smallmatrix}\downarrow\\ \downarrow\end{smallmatrix}\rangle$). Since we are investigating the X^{2-} recombination to the two-electron singlet state, we will thus focus on the antiparallel X^{2-} states being the only two that have nonzero oscillator strength to such a final state.

The exchange interaction between the magnetic ion and the unpaired carriers modifies the energy spectrum of the X^{2-} states according to the following Hamiltonian [11,13,23]:

$$H_{\text{exch}}^{\text{ion}} = A_e^p \vec{S}\vec{\sigma}^p + A_h^s\left[S_z J_z^s + \epsilon\left(S_x J_x^s + S_y J_y^s\right)\right], \qquad (3)$$

where $\vec{S}$ is the Mn^{2+} spin operator, while A_e^p (A_h^s) is the exchange integral between the ion and the p-shell electron (s-shell hole). The leading term in the above Hamiltonian corresponds to spin-conserving part $A_h^s S_z J_z^s$ of the hole-ion exchange, which does not couple the antiparallel and parallel states of the X^{2-}. However, such a coupling arises due to the off-diagonal terms of the electron-ion exchange or the terms related to the valence-band mixing (described by the parameter ϵ in $H_{\text{exch}}^{\text{ion}}$). As proven by our experiments, the amplitude of both effects is relatively small, first due to the presence of δ_0^{ps} splitting, and second due to negligible values of A_e^p and ϵ. Consequently, in the first stage we will simply neglect the off-diagonal terms in the $H_{\text{exch}}^{\text{ion}}$ (their influence will be discussed in Sec. IV). Within such an approximation, the effect of the carrier-ion exchange on the X^{2-} states can be described in terms of an effective longitudinal magnetic-field picture. The value of such a field is proportional to the ion spin projection on the growth axis z. This effective field introduces a Zeeman-like splitting between pure antiparallel X^{2-} spin states associated with the same ion spin projection S_z. Such a splitting competes with the anisotropic splitting δ_1^{ps} leading to six pairs of eigenstates $|\psi_\pm, S_z\rangle$ corresponding to different S_z. Each of these pairs takes on the form

$$|\psi_+, S_z\rangle = \cos(\theta)\left|\begin{smallmatrix}\downarrow\\ \uparrow\downarrow\end{smallmatrix}\Uparrow, S_z\right\rangle + \sin(\theta)\left|\begin{smallmatrix}\uparrow\\ \uparrow\downarrow\end{smallmatrix}\Downarrow, S_z\right\rangle, \qquad (4)$$

$$|\psi_-, S_z\rangle = \cos(\theta)\left|\begin{smallmatrix}\uparrow\\ \uparrow\downarrow\end{smallmatrix}\Downarrow, S_z\right\rangle - \sin(\theta)\left|\begin{smallmatrix}\downarrow\\ \uparrow\downarrow\end{smallmatrix}\Uparrow, S_z\right\rangle, \qquad (5)$$

where the notation exploiting the angle θ is used after Refs. [22,38] with θ defined by $\tan(2\theta) = \delta_1^{ps}/(\delta_{\text{Mn}} S_z)$ for $\delta_{\text{Mn}} = 3A_h^s - A_e^p$. Since the time-reversal symmetry is preserved in the absence of the magnetic field, the $|\psi_\pm, \pm S_z\rangle$ states are degenerate for a given S_z. Consequently, we are left with six twofold-degenerate energy levels associated with the antiparallel X^{2-} states, as shown in Fig. 2. The optical transitions from each of these levels to the singlet final state have equal oscillator strength, however they exhibit different linear polarization degrees determined by $\sin(2\theta)$. The energy splitting between the pairs of levels corresponding to the same $|S_z|$ yields

$$\Delta E(|S_z|) = \sqrt{\Delta^2 + (\delta_{\text{Mn}} S_z)^2} \qquad (6)$$

for $\Delta = \delta_1^{ps}$. Such a formula describes also the energies of the bright states of the neutral exciton in Mn-doped QD [22], in which case $\Delta = \delta_1$ corresponds to the anisotropic exchange between the s-shell hole and the s-shell electron. Since δ_1 is typically much smaller than δ_{Mn}, six X emission lines are almost equidistant. On the other hand, for X^{2-} the value of δ_1^{ps} is comparable with δ_{Mn}. As a result, it strongly influences the energy splitting, leading to the presence of the aforementioned gap between three higher- and three lower-energy X_s^{2-} emission lines.

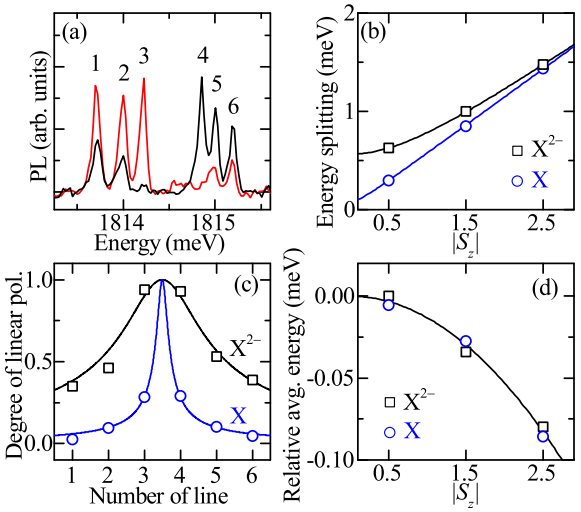

FIG. 3. (Color online) (a) The PL spectra corresponding to the X^{2-} recombination to the singlet final state measured for the QD1. Black and red (gray) curves represent the spectra detected in two orthogonal linear polarizations, the orientations of which correspond to principal axes of δ_1^{ps} anisotropy. The lines of consecutive energies correspond to the absolute values of the ion spin projections $|S_z|$ of 5/2, 3/2, 1/2, 1/2, 3/2, and 5/2. (b) Energy splitting between the pairs of emission lines vs $|S_z|$ for both X^{2-} and X. The solid lines represent the fitted curves described by Eq. (6). (c) Linear polarization degrees (absolute values) of consecutive emission lines of X^{2-} and X compared with the theoretical predictions (solid lines). The experimental values were determined by fitting six Gaussian profiles to X^{2-} or X PL spectra measured for a whole range of orientations of detected linear polarization. (d) Relative average energies of the pairs of PL lines corresponding to the same $|S_z|$ for both X^{2-} and X. The solid line represents the fitted curve of the form ηS_z^2 with $\eta = -13$ μeV.

All of the above theoretical predictions are fully confirmed by the results of our measurements of the energies and polarization properties of the X^{2-} optical transitions to the singlet final state. The two X^{2-} PL spectra detected in orthogonal linear polarizations are shown in Fig. 3(a). The splittings between the pairs of X^{2-} lines associated with the same $|S_z|$ are presented in Fig. 3(b), in which they are compared with analogous splittings obtained for the neutral exciton. In both cases, the experimental data are aptly reproduced by the formula given by Eq. (6). On this basis, we determine both $|\delta_1^{ps}| = 560$ μeV and $|\delta_1| = 85$ μeV for the QD1, which are consistent with the results of previous studies of nonmagnetic CdTe QDs [30]. Apart from the large anticipated difference between δ_1^{ps} and δ_1, the values of δ_{Mn} obtained for both complexes are very similar, yielding 545 and 570 μeV for the X^{2-} and X, respectively. This result directly reflects the similar nature of the ion-related splitting in both cases, which is dominated by the exchange interaction between the ion and the *s*-shell hole.

The relatively large anisotropy of intershell electron-hole exchange entails also partial linear polarization of X^{2-} emission lines, which is clearly visible in Fig. 3(a). The linear polarization degrees determined for consecutive PL lines are shown in Fig. 3(c). Their values are governed by the interplay between δ_1^{ps} anisotropy and the ion-related effective magnetic field. The former effect dominates for the inner X^{2-} energy levels (related to $|S_z| = 1/2$), which underlies the almost total linear polarization of the corresponding emission lines. For larger values of $|S_z|$, the ion-related Zeeman-like splitting becomes stronger, which leads to a decreased linear polarization degree of the outer X^{2-} emission lines. An effect of a similar nature occurs also for the neutral exciton [22], but the polarization degrees of respective emission lines are significantly lower due to much smaller δ_1 anisotropy [see Fig. 3(c)]. According to the theoretical model, the linear polarization degrees of the PL lines related to both excitonic complexes are quantitatively described by $\Delta/\sqrt{\Delta^2 + (\delta_{\mathrm{Mn}} S_z)^2}$, where Δ equals either δ_1^{ps} or δ_1 for X^{2-} or X, respectively. As seen in Fig. 3(c), such a dependence accurately reproduces the experimental results. Importantly, such an agreement is obtained for the same set of parameters previously used to describe the energies of the X and X^{2-} PL lines. This result provides a strong confirmation of the correct identification of the relevant effects determining the X^{2-} fine structure.

However, a closer examination of the X^{2-} PL spectra from Fig. 3(a) reveals also the presence of some additional irregularities in spacing of the emission lines. In particular, the energy distance between lines 1 and 2 is clearly larger than the distance between lines 5 and 6. Such an effect indicates a difference between the average energies of the pairs of X^{2-} states corresponding to the same $|S_z|$. Indeed, as shown in Fig. 3(d), these average energies are decreasing for larger $|S_z|$. The same effect is observed also for the neutral exciton and was previously interpreted in terms of the perturbation of the hole wave function imposed by the hole-ion exchange interaction [21,36,37,39]. Such a perturbation can be described by an effective Hamiltonian $H_{\mathrm{conf}} = \eta S_z^2$. As seen in Fig. 3(d), such a Hamiltonian correctly reproduces the average energies of respective pairs of emission lines for both X and X^{2-}. In both cases, the value of proportionality constant η is the same within the experimental accuracy, which is expected for excitonic complexes containing a single *s*-shell hole.

IV. MAGNETO-PL OF X^{2-} IN Mn-DOPED QD

As we have demonstrated, the zero-field properties of the X^{2-} emission to the two-electron singlet state are described by the same formulas as for the neutral exciton, in spite of the microscopic difference between both complexes. Such a difference is effectively encapsulated in the relatively larger value of the anisotropy parameter for the X^{2-}. However, more distinct differences between both complexes become apparent from an analysis of the X^{2-} PL spectrum evolution in magnetic field applied in a Faraday configuration. A typical result of such an experiment is presented in Fig. 4(a). The general appearance is again similar to the case of the neutral exciton [11,21–23], and it can be described by extending the X^{2-} Hamiltonian from Eq. (1) with the Zeeman terms related to the Mn^{2+} ion and each confined carrier. In the case of the final two-electron states of the X^{2-} recombination, their singlet-triplet structure is almost not affected by the magnetic field <10 T, since the corresponding Zeeman energies are much smaller than the electron-electron exchange integral [28]. Therefore, the only factor influencing the energies of the electron-singlet final states is the ion Zeeman effect, which is identical as in case

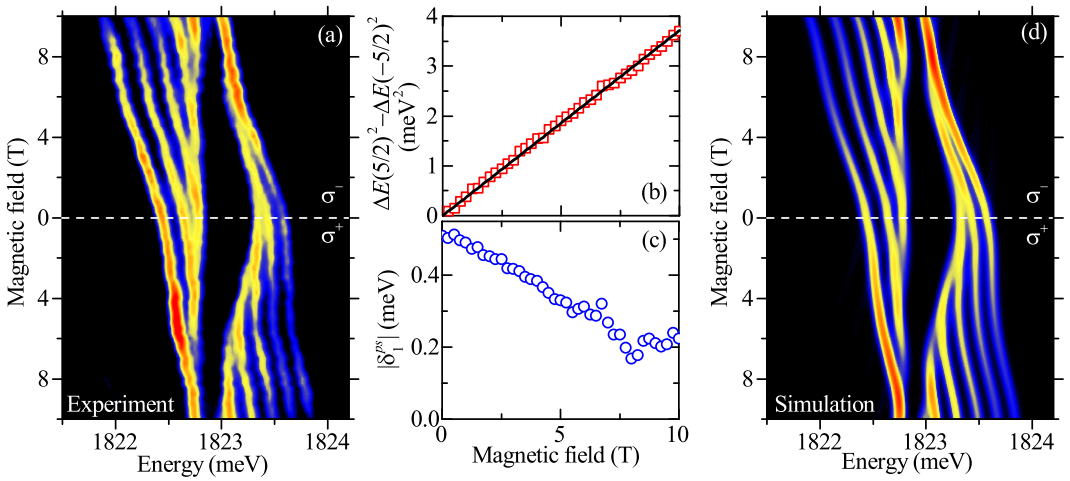

FIG. 4. (Color online) (a) Magnetic field dependence of the PL spectrum related to the X^{2-} recombination to the two-electron singlet state measured for the QD2. The spectra were detected in σ^+ and σ^- circular polarizations (as indicated). (b) The difference between squared energy splittings of the pairs of X^{2-} emission lines associated with the ion spin projections of 5/2 and $-5/2$ in a magnetic field. The solid line represents the linear fit. (c) The value of δ_1^{ps} determined for different values of the magnetic field. (d) Theoretical simulation of the X^{2-} PL spectrum evolution in a magnetic field.

of the initial X^{2-} states. As a consequence, such an effect does not affect the energies of the X^{2-} optical transitions, which are preserving the ion spin projection. The PL lines are thus split only by the Zeeman terms related to the unpaired carriers from the antiparallel X^{2-} states. This leads to the presence of two branches of X^{2-} emission lines observed in opposite circular polarizations. Each of these branches, as seen in Fig. 4(a), closely resembles the zero-field X^{2-} PL spectrum and consists of six emission lines. The lines of consecutive energies correspond to ion spin projections S_z ranging from $\mp 5/2$ to $\pm 5/2$ in $\sigma^{\pm}$ polarization. The energy splitting between the pair of lines related to a given S_z is modified with respect to the zero-field splitting from Eq. (6) by the Zeeman shift of the antiparallel X^{2-} states, and it yields

$$\Delta E(S_z, B) = \sqrt{\left(\delta_1^{ps}\right)^2 + (\delta_{\mathrm{Mn}} S_z + g\mu_B B)^2}, \qquad (7)$$

where $g = 3g_h^s - g_e^p$ is the effective excitonic g factor, with g_h^s and g_e^p being the g factors of the s-shell hole and the p-shell electron, respectively. For the pairs of lines associated with $S_z > 0$, the Zeeman term $g\mu_B B$ increases the splitting of $\delta_{\mathrm{Mn}} S_z$ related to the carrier-ion exchange interaction. Consequently, the linear field dependence of the corresponding emission energies is only slightly perturbed by δ_1^{ps}, as observed for three higher-energy (lower-energy) lines in σ^+ (σ^-) polarization. The opposite effect occurs in the case of three remaining pairs of lines related to $S_z < 0$, for which the excitonic Zeeman splitting counteracts the ion-related exchange splitting. At magnetic fields close to $B = \delta_{\mathrm{Mn}}|S_z|/g\mu_B$, these two effects compensate and the anisotropic electron-hole exchange becomes a dominant source of the splitting. This gives rise to relatively wide anticrossings, which appear in both circular polarizations as a central gap in the emission spectra. For the studied QD, only the anticrossings between the lines related to $S_z = -1/2$ and $-3/2$ are observed at $B = 2$ T and 6.5 T, whereas the anticrossing of the lines corresponding to $S_z = -5/2$ is expected to occur at about 11 T. Within a simple model, the energy splitting at each of these anticrossings should be the same and equal to δ_1^{ps}. On the contrary, the energy width of the central gap in Fig. 4(a) clearly diminishes for larger fields. This result proves unequivocally that the strength of the intershell electron-hole exchange interaction varies with the magnetic field. To the best of our knowledge, such an effect has not been observed experimentally for δ_1 exchange interaction in the case of the neutral exciton, nor has it been predicted theoretically for any other excitonic complex.

To determine the actual values of δ_1^{ps} at various magnetic fields, we analyze the energy splittings between two pairs of outermost X^{2-} PL lines associated with $S_z = 5/2$ and $-5/2$. None of these lines is involved in the anticrossing in the studied field range, which allows us to precisely determine their energies based on the data from Fig. 4(a). We first focus on the difference between squared energy splittings $\Delta E(5/2, B)^2 - \Delta E(-5/2, B)^2$, which is shown in Fig. 4(b). According to Eq. (7), such a difference should exhibit a linear field dependence with a slope independent of δ_1^{ps} and defined by $10\delta_{\mathrm{Mn}} g\mu_B$. This prediction is perfectly reproduced by the experimental data, which confirms that neither the ion-related exchange splitting δ_{Mn} nor the excitonic g factor is affected by the magnetic field. The linear fit together with the analysis of the zero-field splitting of X^{2-} emission lines enable us to independently obtain the values of both δ_{Mn} and g. By substituting them into Eq. (7), we extract the field dependence of δ_1^{ps} from the measured energy splittings between the pairs of X^{2-} lines associated with $S_z = \pm 5/2$. The obtained dependence is presented in Fig. 4(c). As previously indicated, we observe a clear decrease of $|\delta_1^{ps}|$ with the magnetic field. The decrease is almost linear with a slope of $\alpha(\delta_1^{ps}) \approx -35$ μeV/T, which corresponds to a reduction of $|\delta_1^{ps}|$ to about 40% of its zero-field value at $B = 10$ T. The physical origin of the observed variation of δ_1^{ps} is most probably related to the modification of the carrier wave function induced by the magnetic field. From this point of view, a relatively large change of δ_1^{ps} splitting confirms that the dominant contribution to this splitting comes from the

long-range intershell electron-hole exchange interaction [35,40,41], as only this contribution is sensitively dependent on the actual shape of the carrier wave function. Interestingly, signatures of the δ_1^{ps} field dependence appear also in the experimental data obtained previously for nonmagnetic CdTe QDs, which were presented in Fig. 5(b) of Ref. [28]. However, in the absence of the magnetic ion, the X^{2-} emission to the singlet state consists of only two lines, and the splitting between them does not provide sufficient information to unequivocally identify the effect of δ_1^{ps} variation with the magnetic field.

The above-determined parameters characterizing the X^{2-}-Mn^{2+} complex are obtained solely from the energies of X^{2-} PL lines related to $S_z = \pm 5/2$. To demonstrate that the same parameters can be also used to describe the magnetic field dependence of the whole X^{2-} PL spectrum, we perform a numerical simulation of the expected field evolution. The energies of X^{2-} optical transitions to the electron-singlet final states are computed based on numerical diagonalization of the previously introduced X^{2-} Hamiltonian. It describes the spin properties of the X^{2-} complex, but it does not account for effects such as the diamagnetic shift. Therefore, to facilitate the comparison with the experimental data, we include in our calculations a phenomenological shift of the mean X^{2-} emission energy in the magnetic field, which is visible in Fig. 4(a). Finally, to reproduce the change of the X^{2-} PL intensities related to field-induced ion spin orientation [11], we also introduce an effective Mn^{2+} spin temperature, which is assumed to be 35 K. The intensity of each X^{2-} emission line is thus calculated as a product of oscillator strength and the Boltzmann term corresponding to occupancy of the Zeeman-split ion spin states. The result of such a simulation performed without additional fitting parameters is presented in Fig. 4(d). A perfect overall agreement with the experiment confirms the self-consistency of our model and correct interpretation of all observed effects.

Remarkably, apart from δ_1^{ps}-related anticrossings, the field dependence of the X^{2-} PL spectrum does not feature any other anticrossing. This observation constitutes a second important difference between the X^{2-} and the neutral exciton, as in the latter case several additional anticrossings typically appear at various magnetic fields [11,21–23]. In the particular case of the studied QD, the X magneto-PL presented in Fig. 5(a) demonstrates five anticrossings visible around $B = 6$ T in σ^- circular polarization. Each of them involves a bright exciton corresponding to the ion spin projection of $S_z < 5/2$ and a dark exciton with the ion spin projection increased by 1. Such states are coupled by isotropic electron-Mn^{2+} exchange interaction, which gives rise to the observed anticrossings when the zero-field splitting δ_0 between bright and dark states is compensated by the Zeeman effect. The energy splitting at each of the anticrossings is thus directly related to the exchange integral A_e^s between the s-shell electron and the Mn^{2+} ion, which is determined to be about -60 μeV for the presented dot. In general, another set of anticrossings could also arise due to the hole-Mn^{2+} exchange in the presence of the valence-band mixing [23,25], however the strength of this mixing was found to be negligible in the case of the studied QD.

Anticrossings of a similar nature are also expected to occur for the X^{2-}. In such a case, there are naturally no dark states, however their role is played by the X^{2-} states with

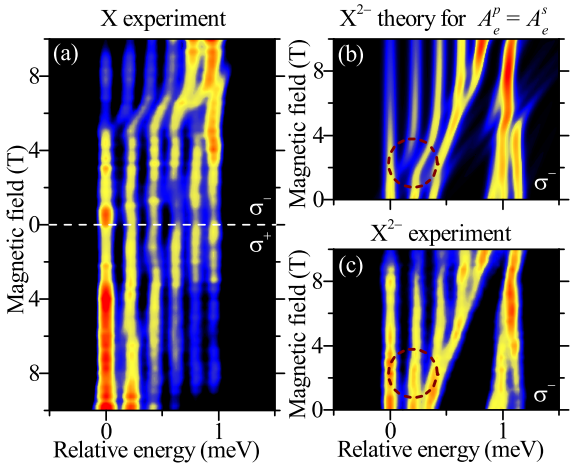

FIG. 5. (Color online) (a) Magnetic field dependence of the neutral exciton PL spectrum for the QD2 detected in two circular polarizations. (b) The simulation of the field evolution of X^{2-} PL spectrum in σ^- polarization under an assumption that the exchange interaction between the Mn^{2+} ion and the p-shell electron is equally strong as the ion exchange with the s-shell electron. In the calculation, we used $\delta_0^{ps} = 0.3$ meV and $g_e^p = -0.2$, while all other parameters were the same as for the simulation presented in Fig. 4(d). (c) The actual σ^- polarized magneto-PL of the X^{2-} measured for the QD2. For better visibility of the anticrossings, in the case of each presented map, the energy axes of the PL spectra were shifted depending on the magnetic field, so that the relative energy of the leftmost emission line is the same for all fields.

a parallel orientation of p-shell electron and s-shell hole spins (see Fig. 2). As was shown in Sec. III, such states cannot recombine to the two-electron singlet state as long as they are not mixed with the antiparallel X^{2-} states. This mixing is induced by the exchange interaction $A_e^p \vec{S}\vec{\sigma}^p$ between the Mn^{2+} ion and the p-shell electron, which should result in a series of anticrossings in the X^{2-} magneto-PL. Importantly, given that the structure of the X^{2-} and X Hamiltonians is exactly the same, the difference between the anticrossings observed in both cases stems only from different values of the Hamiltonian parameters. In particular, the anticrossings for the X^{2-} are expected to occur at lower magnetic fields due to smaller zero-field splitting between antiparallel and parallel X^{2-} states, $\delta_0^{ps} < \delta_0$. More specifically, neglecting the effects of the anisotropic electron-hole exchange, the field corresponding to the anticrossing between $|\begin{smallmatrix}\uparrow\\ \uparrow\downarrow\end{smallmatrix} \Downarrow, S_z\rangle$ and $|\begin{smallmatrix}\downarrow\\ \uparrow\downarrow\end{smallmatrix} \Downarrow, S_z+1\rangle$ states of X^{2-} can be expressed as

$$B_a(S_z) = \frac{\delta_0^{ps} + \frac{1}{2}\delta_{\mathrm{Mn}} + A_e^p(S_z+1)}{\left(g_{\mathrm{Mn}} - g_e^p\right)\mu_B}, \tag{8}$$

where $g_{\mathrm{Mn}} = 2.0$ is the g factor of the Mn^{2+} ion [20,42,43]. Using typical values of $\delta_0^{ps} = 0.3$ meV and $|g_e^p| \ll g_{\mathrm{Mn}}$ for CdTe QDs [30,44] as well as assuming that $|A_e^p| \leqslant |A_e^s|$, we obtain the expected values of B_a for the studied QD. They vary from about 2 to 5 T, and thus they remain in the experimentally accessible range. This simple analysis is confirmed by exact numerical simulation of the X^{2-} magneto-PL performed for an overestimated value of A_e^p equal to A_e^s. The result of such simulation is presented in Fig. 5(b). The anticrossings between

TABLE I. The values of the parameters describing the carrier-ion and intershell electron-hole exchange interactions for the X^{2-} complex determined for five different CdTe/ZnTe QDs containing single Mn^{2+} ions (in the case of the QD1, only the zero-field properties were analyzed). The carrier-ion exchange integrals for the X are provided for reference. The exchange energies are given in μeV, while the slope $\alpha(\delta_1^{ps})$ of $|\delta_1^{ps}|$ decrease with the magnetic field is expressed in μeV/T.

	X^{2-}				X	
	A_h^s	$\lvert A_e^p\rvert$	$\lvert\delta_1^{ps}(0\ \mathrm{T})\rvert$	$\alpha(\delta_1^{ps})$	A_h^s	A_e^s
QD1	$3A_h^s - A_e^p = 545$		560	–	$3A_h^s - A_e^s = 570$	
QD2	134	<20	510	−35	107	−60
QD3	206	<30	470	−20	99	−95
QD4	134	<30	450	−20	126	−55
QD5	203	<35	550	−10	182	−90

antiparallel and parallel X^{2-} states are distinctly visible in the anticipated field range. They are particularly clear for the PL lines with the field evolution only slightly affected by δ_1^{ps}. For example, in the case of the emission line related to $S_z = 3/2$, a pronounced anticrossing appears at about 2.5 T [it is marked by a circle in Fig. 5(b)]. The absence of this anticrossing in the actual experimental data from Fig. 5(c) is a direct fingerprint of the negligible strength of the exchange interaction between the Mn^{2+} ion and the p-shell electron. The analysis of the energy width of the studied PL line in the field range corresponding to the expected anticrossing allows us to provide an upper bound for $|A_e^p| < 20\ \mu$eV, which is three times smaller than $|A_e^s|$ previously determined from the X magneto-PL. This finding implies that the density of the p-shell electronic wave function at the position of the ion is significantly smaller than the density of the s-shell wave function [26]. Such a difference results from the qualitatively different symmetries of these two wave functions. In particular, the s-shell wave function has an antinode at the center of the dot, while the p-shell wave function has a node. Consequently, the negligible density of the latter wave function at the Mn^{2+} site clearly indicates that the ion is approximately centrally localized in the studied QD.

All of the main findings of our analysis were independently confirmed for several Mn-doped QDs. The parameters describing the X^{2-} and the X determined for all dots are summarized in Table I. We stress that in the case of each dot studied in the magnetic field, the measured X^{2-} magneto-PL revealed two characteristic features demonstrated previously for the QD2, namely a close-to-linear field-induced decrease of $|\delta_1^{ps}|$ and a negligible value of the Mn^{2+} exchange integral with the p-shell electron. The former effect is most likely independent of the presence of the ion in the dot and may be considered representative for the studied CdTe/ZnTe QD system. On the other hand, the central position of the ion in the investigated dots evidenced by $|A_e^p| \ll |A_e^s|$ is likely to be related to the employed QD selection procedure, which is aimed at finding dots exhibiting possibly large ion-related splitting of X emission lines.

The detailed analysis of the data from Table I reveals also a notable difference between hole-Mn^{2+} exchange integrals for the X^{2-} and the neutral exciton. In the former case, the integral is systematically larger for each studied QD, despite the fact that for both excitonic complexes the hole occupies the same orbital state. A similar difference in strength of the hole-Mn^{2+} coupling was previously observed for singly charged excitons [24]. The origin of this effect is related to the relatively weak confinement of the hole in a CdTe/ZnTe QD, which can be significantly increased by the Coulomb interaction with the electrons residing in the dot. Such additional hole localization due to the Coulomb attraction is naturally larger for the X^{2-}, resulting in an increased density of the hole wave function at the position of the centrally localized Mn^{2+} ion in a dot.

V. CONCLUSIONS

We conclude that regarding the transitions to the singlet final state, the X^{2-}-Mn^{2+} complex is formally fully equivalent to the neutral exciton in Mn-doped QD. Simultaneously, different values of the exchange parameters for the X^{2-} open the possibility to explore a regime that is not available in the case of the neutral exciton. For example, the exchange interaction between the X^{2-} and the Mn^{2+} ion located in the center of a QD was shown to be completely determined by the hole-Mn^{2+} exchange, as the Mn^{2+} exchange with the p-shell electron was demonstrated to be negligible. Such a result indicates that simultaneous flips of electron and Mn^{2+} spins (flip-flops) for the X^{2-} should be strongly hindered as compared to the X, which in turn may result in different Mn^{2+} spin dynamics induced by both complexes.

By taking advantage of the presence of a Mn^{2+} ion in a QD and the resulting splitting of the X^{2-} emission energies, we were also able to significantly extend the knowledge of the excitons in QDs. In particular, detailed analysis of the magnetic field dependence of the X^{2-} PL spectrum allowed us to identify a pronounced field-induced decrease of the value of $|\delta_1^{ps}|$ exchange constant, which was impossible for nonmagnetic QDs. Moreover, the strength of the hole-Mn^{2+} exchange was used as a tool to evaluate the local density of the hole wave function in a QD. On this basis, we evidenced that the hole localization for the X^{2-} complex may be significantly increased as compared to the X, which is a result of the Coulomb interaction with two additional resident electrons.

ACKNOWLEDGMENTS

This work was supported by the Polish National Science Centre under decisions DEC-2012/07/N/ST3/03130 and DEC-2011/02/A/ST3/00131; by the Polish Ministry of Science and Higher Education in years 2012–2016 as a research

grant "Diamentowy Grant"; and by the Foundation for Polish Science (FNP) subsidy "Mistrz." The project was carried out with the use of CePT, CeZaMat, and NLTK infrastructures financed by the European Union–the European Regional Development Fund within the Operational Programme "Innovative economy" for 2007–2013.

[1] D. Gammon, E. S. Snow, B. V. Shanabrook, D. S. Katzer, and D. Park, Fine structure splitting in the optical spectra of single GaAs quantum dots, Phys. Rev. Lett. **76**, 3005 (1996).

[2] V. D. Kulakovskii, G. Bacher, R. Weigand, T. Kümmell, A. Forchel, E. Borovitskaya, K. Leonardi, and D. Hommel, Fine structure of biexciton emission in symmetric and asymmetric CdSe/ZnSe single quantum dots, Phys. Rev. Lett. **82**, 1780 (1999).

[3] L. Besombes, K. Kheng, and D. Martrou, Exciton and biexciton fine structure in single elongated islands grown on a vicinal surface, Phys. Rev. Lett. **85**, 425 (2000).

[4] M. Bayer, G. Ortner, O. Stern, A. Kuther, A. A. Gorbunov, A. Forchel, P. Hawrylak, S. Fafard, K. Hinzer, T. L. Reinecke, S. N. Walck, J. P. Reithmaier, F. Klopf, and F. Schäfer, Fine structure of neutral and charged excitons in self-assembled In(Ga)As/(Al)GaAs quantum dots, Phys. Rev. B **65**, 195315 (2002).

[5] O. Benson, C. Santori, M. Pelton, and Y. Yamamoto, Regulated and entangled photons from a single quantum dot, Phys. Rev. Lett. **84**, 2513 (2000).

[6] R. J. Young, R. M. Stevenson, A. J. Shields, P. Atkinson, K. Cooper, D. A. Ritchie, K. M. Groom, A. I. Tartakovskii, and M. S. Skolnick, Inversion of exciton level splitting in quantum dots, Phys. Rev. B **72**, 113305 (2005).

[7] K. Kowalik, O. Krebs, A. Golnik, J. Suffczyński, P. Wojnar, J. Kossut, J. A. Gaj, and P. Voisin, Manipulating the exciton fine structure of single CdTe/ZnTe quantum dots by an in-plane magnetic field, Phys. Rev. B **75**, 195340 (2007).

[8] R. M. Stevenson, R. J. Young, P. Atkinson, K. Cooper, D. A. Ritchie, and A. J. Shields, A semiconductor source of triggered entangled photon pairs, Nature (London) **439**, 179 (2006).

[9] N. Akopian, N. H. Lindner, E. Poem, Y. Berlatzky, J. Avron, D. Gershoni, B. D. Gerardot, and P. M. Petroff, Entangled photon pairs from semiconductor quantum dots, Phys. Rev. Lett. **96**, 130501 (2006).

[10] R. J. Young, R. M. Stevenson, P. Atkinson, K. Cooper, D. A. Ritchie, and A. J. Shields, Improved fidelity of triggered entangled photons from single quantum dots, New J. Phys. **8**, 29 (2006).

[11] L. Besombes, Y. Léger, L. Maingault, D. Ferrand, H. Mariette, and J. Cibert, Probing the spin state of a single magnetic ion in an individual quantum dot, Phys. Rev. Lett. **93**, 207403 (2004).

[12] A. Kudelski, A. Lemaître, A. Miard, P. Voisin, T. C. M. Graham, R. J. Warburton, and O. Krebs, Optically probing the fine structure of a single Mn atom in an InAs quantum dot, Phys. Rev. Lett. **99**, 247209 (2007).

[13] J. Kobak, T. Smoleński, M. Goryca, M. Papaj, K. Gietka, A. Bogucki, M. Koperski, J.-G. Rousset, J. Suffczyński, E. Janik, M. Nawrocki, A. Golnik, P. Kossacki, and W. Pacuski, Designing quantum dots for solotronics, Nat. Commun. **5**, 3191 (2014).

[14] J. A. Gaj and J. Kossut, in *Introduction to the Physics of Diluted Magnetic Semiconductors*, Springer Series in Materials Science Vol. 144, edited by J. A. Gaj and J. Kossut (Springer, Heidelberg, 2010), pp. 1–36.

[15] C. Le Gall, L. Besombes, H. Boukari, R. Kolodka, J. Cibert, and H. Mariette, Optical spin orientation of a single manganese atom in a semiconductor quantum dot using quasiresonant photoexcitation, Phys. Rev. Lett. **102**, 127402 (2009).

[16] M. Goryca, T. Kazimierczuk, M. Nawrocki, A. Golnik, J. A. Gaj, P. Kossacki, P. Wojnar, and G. Karczewski, Optical manipulation of a single Mn spin in a CdTe-based quantum dot, Phys. Rev. Lett. **103**, 087401 (2009).

[17] C. Le Gall, R. S. Kolodka, C. L. Cao, H. Boukari, H. Mariette, J. Fernández-Rossier, and L. Besombes, Optical initialization, readout, and dynamics of a Mn spin in a quantum dot, Phys. Rev. B **81**, 245315 (2010).

[18] E. Baudin, E. Benjamin, A. Lemaître, and O. Krebs, Optical pumping and a nondestructive readout of a single magnetic impurity spin in an InAs/GaAs quantum dot, Phys. Rev. Lett. **107**, 197402 (2011).

[19] T. Smoleński, W. Pacuski, M. Goryca, M. Nawrocki, A. Golnik, and P. Kossacki, Optical spin orientation of an individual Mn^{2+} ion in a CdSe/ZnSe quantum dot, Phys. Rev. B **91**, 045306 (2015).

[20] M. Goryca, M. Koperski, P. Wojnar, T. Smoleński, T. Kazimierczuk, A. Golnik, and P. Kossacki, Coherent precession of an individual 5/2 spin, Phys. Rev. Lett. **113**, 227202 (2014).

[21] L. Besombes, Y. Léger, L. Maingault, D. Ferrand, H. Mariette, and J. Cibert, Carrier-induced spin splitting of an individual magnetic atom embedded in a quantum dot, Phys. Rev. B **71**, 161307 (2005).

[22] Y. Léger, L. Besombes, L. Maingault, D. Ferrand, and H. Mariette, Geometrical effects on the optical properties of quantum dots doped with a single magnetic atom, Phys. Rev. Lett. **95**, 047403 (2005).

[23] M. Goryca, P. Plochocka, T. Kazimierczuk, P. Wojnar, G. Karczewski, J. A. Gaj, M. Potemski, and P. Kossacki, Brightening of dark excitons in a single CdTe quantum dot containing a single Mn^{2+} ion, Phys. Rev. B **82**, 165323 (2010).

[24] Y. Léger, L. Besombes, J. Fernández-Rossier, L. Maingault, and H. Mariette, Electrical control of a single Mn atom in a quantum dot, Phys. Rev. Lett. **97**, 107401 (2006).

[25] Y. Léger, L. Besombes, L. Maingault, and H. Mariette, Valence-band mixing in neutral, charged, and Mn-doped self-assembled quantum dots, Phys. Rev. B **76**, 045331 (2007).

[26] M. M. Glazov, E. L. Ivchenko, L. Besombes, Y. Léger, L. Maingault, and H. Mariette, Fine structure of exciton excited levels in a quantum dot with a magnetic ion, Phys. Rev. B **75**, 205313 (2007).

[27] U. C. Mendes, M. Korkusiński, A. H. Trojnar, and P. Hawrylak, Optical properties of charged quantum dots doped with a single magnetic impurity, Phys. Rev. B **88**, 115306 (2013).

[28] T. Kazimierczuk, T. Smoleński, J. Kobak, M. Goryca, W. Pacuski, A. Golnik, K. Fronc, Ł. Kłopotowski, P. Wojnar, and P. Kossacki, Optical study of electron-electron exchange interaction in CdTe/ZnTe quantum dots, Phys. Rev. B **87**, 195302 (2013).

[29] J. Suffczyński, T. Kazimierczuk, M. Goryca, B. Piechal, A. Trajnerowicz, K. Kowalik, P. Kossacki, A. Golnik, K. P. Korona, M. Nawrocki, J. A. Gaj, and G. Karczewski, Excitation mechanisms of individual CdTe/ZnTe quantum dots studied by photon correlation spectroscopy, Phys. Rev. B **74**, 085319 (2006).

[30] T. Kazimierczuk, T. Smoleński, M. Goryca, Ł. Kłopotowski, P. Wojnar, K. Fronc, A. Golnik, M. Nawrocki, J. A. Gaj, and P. Kossacki, Magnetophotoluminescence study of intershell exchange interaction in CdTe/ZnTe quantum dots, Phys. Rev. B **84**, 165319 (2011).

[31] R. J. Warburton, C. Schäflein, D. Haft, F. Bickel, A. Lorke, K. Karrai, J. M. Garcia, W. Schoenfeld, and P. M. Petroff, Optical emission from a charge-tunable quantum ring, Nature (London) **405**, 926 (2000).

[32] J. J. Finley, P. W. Fry, A. D. Ashmore, A. Lemaître, A. I. Tartakovskii, R. Oulton, D. J. Mowbray, M. S. Skolnick, M. Hopkinson, P. D. Buckle, and P. A. Maksym, Observation of multicharged excitons and biexcitons in a single InGaAs quantum dot, Phys. Rev. B **63**, 161305 (2001).

[33] B. Urbaszek, R. J. Warburton, K. Karrai, B. D. Gerardot, P. M. Petroff, and J. M. Garcia, Fine structure of highly charged excitons in semiconductor quantum dots, Phys. Rev. Lett. **90**, 247403 (2003).

[34] M. Ediger, G. Bester, B. D. Gerardot, A. Badolato, P. M. Petroff, K. Karrai, A. Zunger, and R. J. Warburton, Fine structure of negatively and positively charged excitons in semiconductor quantum dots: Electron-hole asymmetry, Phys. Rev. Lett. **98**, 036808 (2007).

[35] E. Poem, J. Shemesh, I. Marderfeld, D. Galushko, N. Akopian, D. Gershoni, B. D. Gerardot, A. Badolato, and P. M. Petroff, Polarization sensitive spectroscopy of charged quantum dots, Phys. Rev. B **76**, 235304 (2007).

[36] A. H. Trojnar, M. Korkusiński, E. S. Kadantsev, P. Hawrylak, M. Goryca, T. Kazimierczuk, P. Kossacki, P. Wojnar, and M. Potemski, Quantum interference in exciton-Mn spin interactions in a CdTe semiconductor quantum dot, Phys. Rev. Lett. **107**, 207403 (2011).

[37] A. H. Trojnar, M. Korkusiński, U. C. Mendes, M. Goryca, M. Koperski, T. Smoleński, P. Kossacki, P. Wojnar, and P. Hawrylak, Fine structure of a biexciton in a single quantum dot with a magnetic impurity, Phys. Rev. B **87**, 205311 (2013).

[38] L. Besombes, L. Marsal, K. Kheng, T. Charvolin, L. S. Dang, A. Wasiela, and H. Mariette, Fine structure of the exciton in a single asymmetric CdTe quantum dot, J. Cryst. Growth **214-215**, 742 (2000).

[39] L. Besombes and H. Boukari, Resonant optical pumping of a Mn spin in a strain-free quantum dot, Phys. Rev. B **89**, 085315 (2014).

[40] A. Franceschetti, L. W. Wang, H. Fu, and A. Zunger, Short-range versus long-range electron-hole exchange interactions in semiconductor quantum dots, Phys. Rev. B **58**, R13367 (1998).

[41] T. Takagahara, Theory of exciton doublet structures and polarization relaxation in single quantum dots, Phys. Rev. B **62**, 16840 (2000).

[42] M. Quazzaz, G. Yang, S. Xin, L. Montes, H. Luo, and J. K. Furdyna, Electron paramagnetic resonance of Mn^{2+} in strained-layer semiconductor superlattices, Solid State Commun. **96**, 405 (1995).

[43] Y. Léger, L. Besombes, L. Maingault, D. Ferrand, and H. Mariette, Hole spin anisotropy in single Mn-doped quantum dots, Phys. Rev. B **72**, 241309 (2005).

[44] T. Kazimierczuk, M. Goryca, P. Wojnar, A. Golnik, M. Nawrocki, and P. Kossacki, Signatures of p-shell electron g-factor in s-shell emission of CdTe/ZnTe quantum dots, Acta Phys. Pol. A **120**, 874 (2011).